Conical Surfaces and Crescent Singularities in Crumpled Sheets

E. Cerda* and L. Mahadevan†
Division of Mechanics and Materials, Mechanical Engineering, Massachusetts Institute of Technology, 77 Massachusetts Avenue, Cambridge, Massachusetts 02139
(Received 14 October 1997)

We analyze the geometry and elasticity of the crescentlike singularity on a crumpled elastic sheet. We give a physical realization of this in terms of a free-boundary contact problem. An analytical solution is given for the universal shape of a developable cone that characterizes the singularity far from the tip, and some of its predictions are qualitatively verified experimentally. We also give a scaling relation for the core size, defined as the region close to the tip of the cone where the sheet is not developable. [S0031-9007(98)05465-9]

PACS numbers: 68.60.Bs, 03.40.Dz, 46.30.Cn

As children, we are taught that to make a cone out of a piece of paper we should start with a circular sheet, cut out a sector along two distinct radii, and then glue these radii by bending the sheet out of the plane. The curvature of the axisymmetric cone so obtained is finite everywhere except at the tip. Without cutting out this sector, it is impossible to make an axisymmetric cone, because the paper will either tear (when it is stretched to preserve axisymmetry) or buckle (when it is compressed for the same reason). This is a reflection of the fact that, for a thin elastic sheet, the energy required for stretching is very large compared to that for bending [1]. However, in situations such as the buckling of cylinders [2] and the crumpling of flat sheets [3], volume restrictions are so large that bending deformations alone cannot account for storage of energy. The energy then becomes localized along a network of ridges [3], along which bending and stretching energies become comparable. The ridges meet at peaks, which are locally conical, but not axisymmetric.

In this Letter we will consider these nonaxisymmetric peaks that correspond to pointlike singularities of elastic surfaces. They are topologically important since they determine the number of ridges and characterize their lengths and, therefore, the volume of the crumpled sheet. Since a single peak has no scale except that of the thickness of the sheet, it must have a universal shape away from the tip. The shape is that of a developable elastic cone [4] which is isometric to the plane almost everywhere so that it can be made by bending a flat sheet without stretching it anywhere except at the tip. However, this alone does not uniquely specify the cone, since it is possible to make a nonaxisymmetric cone in many ways. In order to make this shape unique, we have to specify some boundary conditions that respect the constraint of unstretchability. This is achieved via a simple experimental realization of a developable cone, shown in Fig. 1. A circular transparency is placed on the edge of a circular glass cylinder and pushed into it axially by a force acting along the axis of the cylinder. This is the simplest volume-restricting deformation of a sheet and causes the center of the sheet to move into the cylinder. The excess material due to this motion is tucked in as a fold, and the sheet is then only in partial contact with the edge of the cylinder. This construction leads to a conical surface with reflection symmetry that is developable everywhere except at the tip. The constraint of unstretchability is accommodated by the sheet as it chooses a solution with lower symmetry (Z^2) than the perfect cone. A different experimental realization of a developable cone may be obtained by constraining the transparency to conform to a conical container so that there is continuous contact in the radial direction. Later we will see that this geometry affords the simplest physical interpretation of the problem.

Mathematically, this may be posed as a free-boundary contact problem or a constrained variational inequality. In order to find the shape of this developable cone far from the tip, we have to minimize the bending energy of the sheet subject to the constraint associated with inextensibility and the inequality constraint associated with contact. To describe the sheet we will use cylindrical coordinates (ρ, θ), $-\pi \leq \theta \leq \pi$ so that a vector $\rho \hat{\rho}$

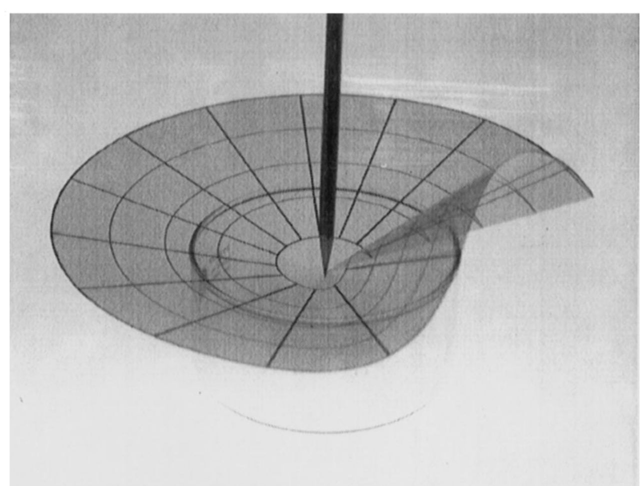

FIG. 1. An experimental realization of a developable cone is accomplished by forcing a circular transparency into a cylindrical glass container.

is deformed into $\vec{r} = \rho\hat{\rho} + u_\rho(\rho,\theta)\hat{\rho} + u_\theta(\rho,\theta)\hat{\theta} + \xi(\rho,\theta)\hat{z}$, where u_ρ, u_θ, and ξ represent the radial, azimuthal, and axial displacements, respectively. Far away from the tip $\rho = 0$, we look for a universal conical solution $\xi = \rho\psi(\theta)$. The condition of inextensibility requires that the stretching strains $\gamma_{\rho\rho}, \gamma_{\rho\theta}, \gamma_{\theta\theta}$, corresponding to moderate deflections [5], vanish in this region, so that

$$\gamma_{\rho\rho} = \partial_\rho u_\rho + \frac{1}{2}(\partial_\rho \xi)^2 = 0,$$
$$\gamma_{\rho\theta} = \frac{1}{2}\left(\frac{\partial_\theta u_\rho}{\rho} + \partial_\rho u_\theta - \frac{u_\theta}{\rho}\right) + \frac{1}{2\rho}\partial_\rho\xi\partial_\theta\xi = 0,$$
$$\gamma_{\theta\theta} = \frac{\partial_\theta u_\theta}{\rho} + \frac{u_\rho}{\rho} + \frac{1}{2\rho^2}(\partial_\theta\xi)^2 = 0. \quad (1)$$

Solving (1) for the radial and the azimuthal displacement yields

$$u_\rho(\rho,\theta) = -\frac{\rho}{2}\psi^2(\theta),$$
$$u_\theta(\rho,\theta) = \frac{\rho}{2}\int^\theta d\theta[\psi^2(\theta) - \psi'^2(\theta)]. \quad (2)$$

Here $(.)' = \partial_\theta(.)$. Then periodicity in the azimuthal direction yields the following condition on ψ:

$$\frac{1}{2}\int_{-\pi}^{\pi} d\theta[\psi^2(\theta) - \psi'^2(\theta)] = 0, \quad (3)$$

which is equivalent to the condition that the Gauss curvature of the developable cone integrated along a contour surrounding the tip vanishes [4]. The inequality constraint corresponding to the requirement that the conical sheet lie inside the cylinder as shown in Fig. 1 is given by

$$\frac{\xi}{\rho} = \psi \geq \epsilon, \quad (4)$$

where $\pi/2 - \tan^{-1}\epsilon$ is the angle of the convex envelope cone. Thus $\xi = \rho\psi(\theta)$ may be determined by minimizing the elastic bending energy of the sheet subject to (3) and (4). To facilitate this, we define the augmented energy functional

$$\mathcal{L}[\psi] = \frac{1}{2}\int_{-\pi}^{\pi} d\theta[\psi''(\theta) + \psi(\theta)]^2 + \frac{\lambda}{2}\int_{-\pi}^{\pi} d\theta[\psi^2(\theta) - \psi'^2(\theta)] + \int_{-\pi}^{\pi} d\theta\, b(\theta)[\epsilon - \psi(\theta)], \quad (5)$$

where the first term is proportional to the bending energy, the second term enforces (3) via the constant Lagrange multiplier λ, and the third term enforces (4) via the Lagrange multiplier $b(\theta)$. Since (4) is an inequality constraint, $b(\theta) > 0$ when $\psi = \epsilon$ and vanishes when $\psi > \epsilon$ [6]. As we will see, λ is proportional to the hoop stress while $b(\theta)$ is proportional to the axial force that maintains the developable cone in equilibrium. The Euler-Lagrange equation for ψ that results from extremizing (5) gives

$$\left(\frac{d^2}{d\theta^2} + a^2\right)\left(\frac{d^2}{d\theta^2} + 1\right)\psi = b, \quad (6)$$

where $a^2 = 1 + \lambda$. As we are looking for a symmetric solution $\psi(\theta) = \psi(-\theta)$, i.e., $\psi = \epsilon$, $|\theta| \geq \theta_1$ and $\psi > \epsilon$, $|\theta| < \theta_1$, where $2\theta_1$ is the angle over which the developable cone is not in contact with the edge of the cylinder. Since $b(\theta)$ vanishes when $|\theta| < \theta_1$, (6) is homogeneous in this region. Then a solution satisfying the continuity conditions $\psi(\pm\theta_1) = \epsilon$ and $\psi'(\pm\theta_1) = 0$ is

$$\Psi(\theta) = \epsilon\left(\frac{\sin\theta_1\cos a\theta - a\sin a\theta_1\cos\theta}{\sin\theta_1\cos a\theta_1 - a\sin a\theta_1\cos\theta_1}\right). \quad (7)$$

Thus the complete solution to (6) is given by

$$\psi(\theta) = \epsilon v(|\theta| - \theta_1) + \Psi(\theta)v(\theta_1 - |\theta|), \quad (8)$$

where $v(x)$ is the usual Heaviside function and the parameters a, θ_1 remain to be found. Substituting (8) into (3) yields

$$\theta_1 D + a\sin\theta_1\sin a\theta_1 - \pi D = \frac{(1 - a^2)}{2D}\sin^2\theta_1\left[\theta_1 + \frac{\sin a\theta_1\cos a\theta_1}{a}\right], \quad (9)$$

where $D = \sin\theta_1\cos a\theta_1 - a\sin a\theta_1\cos\theta_1$. Substituting (8) into (6) yields

$$b(\theta) = \epsilon a^2 v(|\theta| - \theta_1) - \frac{d^3\Psi}{d\theta^3}(\theta)|_{\theta_1}\delta(|\theta| - \theta_1) - \frac{d^2\Psi}{d\theta^2}(\theta)|_{\theta_1}\delta'(|\theta| - \theta_1), \quad (10)$$

where $\delta(x)$ is the Dirac-δ function [7] and $\delta'(x)$ is the derivative of the Dirac-δ function. For the equilibrium solution (8) to be a relative minimum $b(\theta) > 0$, $|\theta| \geq \theta_1$ [6]. Since $\delta(x)$ is a positive even function and $\delta'(x)$ is an odd function, this requires that $a^2 > 0$, $\frac{d^3\Psi}{d\theta^3}|_{\theta_1} < 0$, and from (10) it follows that

$$\frac{d^2\Psi}{d\theta^2}(\theta)|_{\pm\theta_1} = 0. \quad (11)$$

The last condition is tantamount to requiring that the solution has the least possible singularity and is physically equivalent to having no point torques (force dipoles) at $\theta = \pm\theta_1$. Substituting (7) into (11) and simultaneously solving the resulting equation with (9) yields

$$2\theta_1 \approx 2.42 \text{ rad} \approx 140°, \qquad a \approx 3.8. \quad (12)$$

Then $\lambda = 1 + a^2 \approx 13.5$ and the jump $\frac{d^3\Psi}{d\theta^3}|_{\theta_1} \approx -38.7\epsilon$ so that $b(\theta) > 0$, $|\theta| \geq \theta_1$ and the solution is a relative minimum. In Fig. 2, we plot $\xi = \rho\psi(\theta)$ for $\epsilon = 0.1$ showing the shape of the developable cone in the experimental configuration of Fig. 1. In Fig. 3, we depict the generators of the developable cone; these correspond to the lines $\psi'' + \psi = \text{const}$. We observe that the curvature $(\psi'' + \psi)/\rho$ is constant in the cone $(|\theta| \geq \theta_1)$ and changes sign in the invagination in order

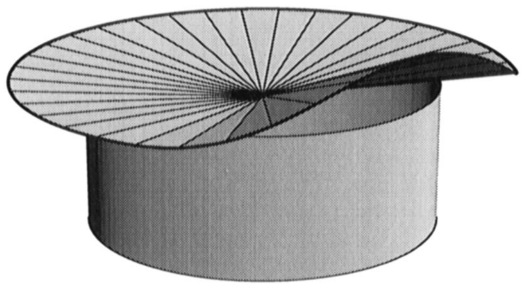

FIG. 2. The developable cone corresponding to Eq. (8) for $\epsilon = 0.1$.

to accommodate the additional circumferential length, while the azimuthal derivative of the curvature is discontinuous along $\theta = \pm\theta_1$, as seen from (10).

To better interpret our solution, we consider the general equation of equilibrium for the transverse displacement ξ of a bent plate [5]

$$B\nabla^4\xi = h\sigma_{\alpha\beta}\partial_\alpha\partial_\beta\xi + P\,. \tag{13}$$

Here $B = Eh^3/12(1 - \nu^2)$ is the bending rigidity, E is Young's modulus, ν is Poisson's ratio, h is the thickness, $\sigma_{\alpha\beta}$ are the in-plane stresses, and P is the axial pressure over the plate. Substituting $\xi = \rho\psi$ into (13) and comparing (6) and (13) term by term, we find that

$$\sigma_{\theta\theta} = -\frac{B\lambda}{h\rho^2}\,, \qquad P = \frac{Bb(\theta)}{h\rho^3}\,. \tag{14}$$

Then $b(\theta) > 0$, $|\theta| \geq \theta_1$ corresponds to an axial external force necessary to maintain the developable cone in equilibrium. This force vanishes when $\psi(\theta) \geq \epsilon$ and is discontinuous at $\theta = \pm\theta_1$ since $b(\theta)$, given in (10), is discontinuous along these two radial lines. We also observe that λ is proportional to the hoop stress in the conical sheet. Thus the simplest interpretation of the nonaxisymmetric solution (8) corresponds to a thin elastic sheet in partial contact with an axisymmetric cone of angle $\pi/2 - \tan^{-1}\epsilon$. Experimentally, the angular opening over which the cone is not in contact with the cylinder is found to be about 130° and compares well with the theoretical prediction $2\theta_1 \sim 140°$. The discontinuity in $b(\theta)$ along $\theta = \pm\theta_1$ implies that the out-of-plane shear stress $Q_\theta = B(\psi''' + \psi')/\rho^2$ [8] is also discontinuous along these two rays. This singularity is amplified by the factor $1/\rho^2$ in Q_θ close to the tip, and ameliorated far from it. This discontinuity occurs because we have neglected out-of-plane shear deformations in our strain measures (1). In thin plate theory, this is known as the Kirchhoff-Love approximation [8] and is violated in a boundary layer of width $O(h)$ [9] over which out-of-plane shear deformations become important. In Fig. 3, we also see that there are two rays along which the curvature is a maximum, with the magnitude increasing as we approach the tip. When the bending stresses along these rays $B(\psi'' + \psi)/\rho$ exceeds the yield stress, the sheet deforms plastically leading to the crescent-shaped scar shown in Fig. 4. From (7), the angular opening of the crescent is found to be $2\theta_0 = 2\pi/a$ rad $\approx 94°$, which compares well with the experimental value of 101° found from Fig. 4.

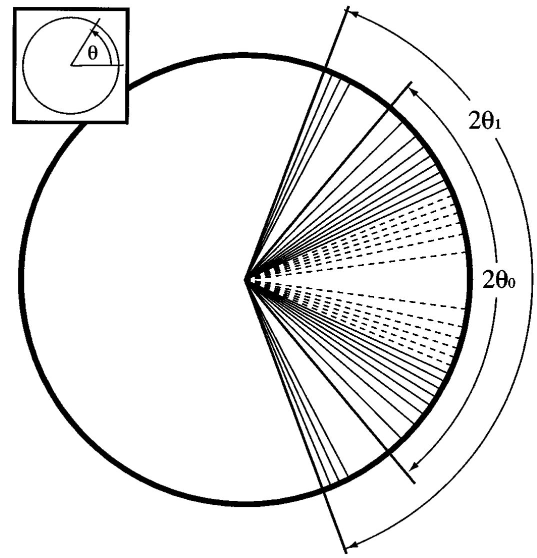

FIG. 3. The generators of the developable cone shown in Fig. 2; the solid lines correspond to $\psi'' + \psi > 0$ and the dotted lines correspond to $\psi'' + \psi < 0$. Here $2\theta_0$ is the angle between the lines of maximum curvature that results in the crescentlike scar and $2\theta_1$ is the angle over which the cone is not in contact with the cylinder.

As ϵ is gradually increased, the developable cone first becomes multivalued. This transition can be predicted in the context of our theory by finding the critical value of $\epsilon_m \sim 0.32$ when the projected angle corresponding to the Monge coordinates gives rise to multivalued ξ. As ϵ is increased still further to $\epsilon_c \sim 0.67$, the cone touches itself along a line (Fig. 5). These values of ϵ do not agree quantitatively with the experimental values of $\epsilon_m \sim 0.5$, $\epsilon_c \sim 0.8$. This is because some quadratic terms in the in-plane stretching which were neglected in the

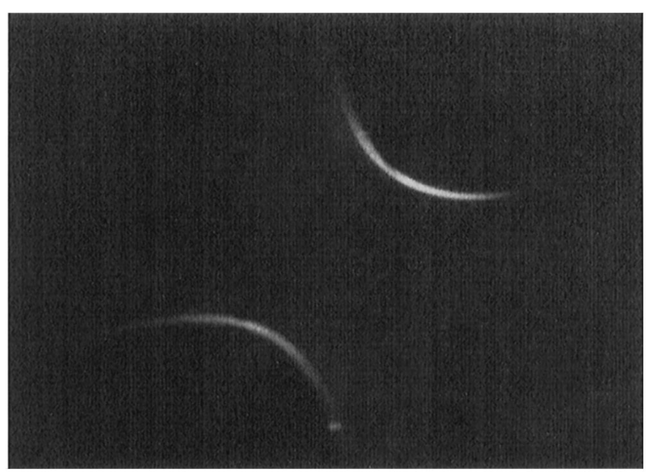

FIG. 4. A closeup view of the scars, one of which is at the tip of the cone in Fig. 1, viewed using reflected light. The whitening is due to plastic deformation.

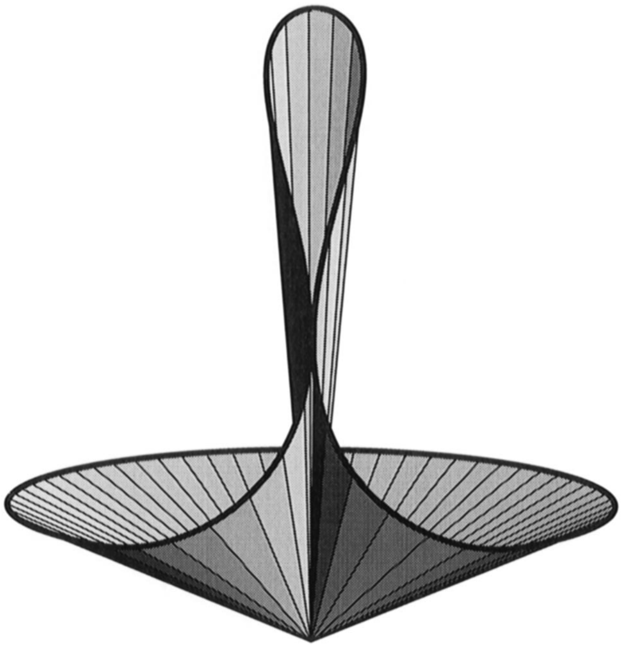

FIG. 5. The shape of the cone for $\epsilon \approx 0.67$ corresponding to the case when the cone touches itself.

weakly nonlinear strain measures (1) become important for moderate ϵ. Their inclusion precludes any analytical insight and yields only quantitative corrections to the above theory.

The solution shown in Fig. 2 may be interpreted as the rotational analog of a macroscopic dislocation at the interface between a thin elastic sheet and a rigid substrate [10]. Here the relative difference between the area of the convex envelope of the sheet and the area of the sheet characterizes the strength of the dislocation. The analogy may be pushed further; the energy of the developable cone is composed of two parts: a bending contribution in the outer region and a stretching and bending contribution near the tip, which is analogous to the core of a dislocation. Since the curvature of the cone is $\kappa \sim \varepsilon/\rho$, the bending energy is $U_b \sim \int_{r_c}^{R} B\kappa^2 \rho\, d\rho = \epsilon^2 B \ln \frac{R}{r_c}$, where r_c is a cutoff radius. This logarithmic divergence and the associated cutoff radius are familiar concepts in dislocation mechanics [11], where r_c is the size of the dislocation core.

We now estimate the dimensions of the core, defined as the region over which the inextensional solution breaks down. As seen in Fig. 4, the core is a crescentlike object whose length far exceeds its width. In fact, there are actually two corelike regions where stretching, plasticity, and other nonlinear effects are important; the first is the long scar itself, and the second is a very small neighborhood of the tip. In this second region of radius $O(h)$, which we call the isotropic core, the assumption of two dimensionality is invalid and one must resort to a full three-dimensional treatment. Radial and circumferential stretching in the first region corresponding to the long crescent are of the same order. Here the deformation of conical wedge into a parabolic profile gives a strain of the order of $1/\cos\epsilon - 1 \sim \epsilon^2$. Then the energy due to stretching is given by $U_s \sim Eh\epsilon^4 r_c^2$. Minimizing the total energy $U_b + U_s$ yields the scaling relation $r_c \sim h/\epsilon$ for the core size. A comparison of these results with experiments [12] will be treated in a future publication.

We thank Y. Pomeau for interesting us in this problem, Dr. C. Mazel of the Edgerton Center, MIT for Fig. 1, 4, and P. Thamburaja for help with some preliminary experiments. E.C. was supported by the Chilean Cátedra Presidencial en Ciencias 1997 Fellowship; L.M. was partially supported by the Sloan Fund at MIT.

*Also affiliated with Centro de Física No-lineal y Sistemas Complejos de Santiago, Chile.
†Electronic address: l_m@mit.edu

[1] Lord Rayleigh, *Theory of Sound* (Dover, New York, 1945), Vol. **I**, Chap. Xa.
[2] T. von Karman and H-S. Tsien, J. Aero Sci. **8**, 303–12 (1941).
[3] A. Lobkovksy, S. Gentges, H. Li, D. Morse, and T. Witten, Science **270**, 1482–84 (1995).
[4] M. Ben Amar and Y. Pomeau, Proc. R. Soc. London A **453**, 729–55 (1997).
[5] L. Landau and E. M. Lifshitz, *Theory of Elasticity* (Pergamon, New York, 1986), 3rd ed.
[6] M. Hestenes, *Calculus of Variations and Optimal Control Theory* (Wiley, New York, 1966).
[7] An interpretation of the Dirac-δ function may be given in the sense of distributions. See M. Lighthill, *An Introduction to Fourier Series and Generalized Functions* (Cambridge University Press, Cambridge, England, 1958).
[8] A. E. H. Love, *A Treatise on the Mathematical Theory of Elasticity* (Dover, New York, 1944).
[9] L. M. Keer and M. A. G. Silva, J. Appl. Mech. **39**, 1121–24 (1972).
[10] E. Orowan, *Dislocations in Metals,* edited by M. Cohen (American Institute of Mining and Metallurgical Engineers, New York, 1954), pp. 359–77; E. Cerda and L. Mahadevan (to be published).
[11] F. R. N. Nabarro, *Theory of Crystal Dislocations* (Dover, New York, 1993).
[12] S. Chaieb, F. Melo, and J-C. Geminard, Phys. Rev. Lett. (to be published).